EUROPEAN ORGANIZATION FOR NUCLEAR RESEARCH

CERN-EP/80-19
19 February 1980

LARGE-ANGLE ELASTIC SCATTERING OF CHARGED PIONS ON PROTONS AT 20 AND 30 GeV/c INCIDENT MOMENTA

R. Almas[5,2], C. Baglin[1], R. Böck[2], E.T.C. Borggaard[3], K. Brobakken[5,2], L. Bugge[5,2], T. Buran[5], A. Buzzo[4], P. Carlson[2], L. Causton[6], M. Coupland[6], D.G. Davis[6], B.G. Duff[6], A. Eide[5], S. Ferroni[4], I. Gjerpe[2], V. Gracco[4], K. Guettler[6], J.P. Guillaud[1], J. Haldorsen[2], J.D. Hansen[3], P. Helgaker[2], F.F. Heymann[6], D.C. Imrie[6], T. Jacobsen[5], K.E. Johansson[2], K. Kirsebom[2], S. Kooijman[6], R. Lowndes[6], A. Lundby[2], G.J. Lush[6], M. Macri[2], R. Møllerud[3], J. Myrheim[2,3,5], M. Poulet[1], L. Rossi[4], A. Santroni[4], B. Schistad[5,2], H. Schwartz[5], G. Skjevling[5,2], S.O. Sørensen[5], J. Tavernier[1], M. Yvert[1]

Annecy (LAPP)[1] - CERN[2] - Copenhagen (Niels Bohr Institute)[3] - Genova[4] - Oslo[5] - University College London[6] Collaboration

ABSTRACT

Elastic cross-section measurements are presented for $\pi^{\pm}$ - p at 20 GeV/c and π^{-} - p at 30 GeV/c incident momenta in the large angle region (50^{o} to 90^{o} in the cm system). The data are compared with lower energy published elastic cross-sections. A test is made of the dimensional counting rules for $\pi^{\pm}$ - p elastic scattering and some indication of a deviation from this rule is observed in the π^{-} - p case. A comparison is also made with the predictions of the constituent interchange model. Although the broad features of the predictions are confirmed, there are some important discrepancies. Finally, the predictions of the model due to Preparata and Soffer are also compared with the new data.

To be submitted to Physics Letter B

January 1980

INTRODUCTION

A series of measurements of elastic hadron-proton scattering at large momentum transfers is in progress at the CERN SPS. This letter reports the first results from large angle scattering of $\pi^+ - p$ at 20 GeV/c and of $\pi^- - p$ at 20 and 30 GeV/c incident momenta. Data are presented in the centre-of-mass angular region from 50° to 90° for $\pi^- - p$ and $\pi^+ - p$ elastic differential cross-sections. The dependence on angle and energy of the cross-section is particularly interesting from the point of view of specific constituent models where definite predictions can be tested. The energy dependence of the differential cross-sections has been studied by combining these new data with previously published large angle cross-sections at lower energies[1].

In order to reach the very small elastic cross-sections expected at large angles, the present measurements were carried out using a very intense secondary beam (typically 5×10^7 particles per machine burst which was 0.8 s in duration), a 1 m long hydrogen target and a large acceptance double arm spectrometer (about 0.1 sr in each arm) to study both scattered particles. The main components of the apparatus are outlined in figure 1.

The beam particles were identified with the help of two differential high pressure gas Cerenkov counters (CEDARS 1 and 2) set to count the two minority components of the beam (K^+ and p or K^- and $\bar{p}$). The position and direction of the incident particle, as it entered the target, were determined with the help of two beam hodoscope units, each of which consisted of three sets of 2 mm wide scintillator strips arranged with one set in the vertical plane and the two sets at $\pm 45^\circ$ to the vertical. Before entering the CEDARS, the beam was made parallel with a divergence of less than 0.15 mrad, and blown up into a large cross-sectional area (about 5 by 2.5 cm^2) so that each hodoscope element had a sufficiently low counting rate not to be saturated. A third differential Cerenkov counter (CEDAR 3) was placed downstream of the target to detect non-interacting minority beam particles accompanying the scattered particle in this intense beam, during the resolving time of the fast electronics.

(This was of particular importance in obtaining the $K^{\pm}$ - p elastic differential cross-sections presented as a separate letter[11]).

The trajectories of the scattered particles were determined by using 6 sets of multiwire proportional planes (CH1 - CH6) in the spectrometer arms. A magnet with an aperture of 150 x 75 cm^2 and a mean integrated field strength of 2.3 Tm was used to determine momenta (p) with a resolution $\Delta p/p = 0.3\% p$ (p in GeV/c). The scattered particles were identified with pairs of threshold atmospheric gas Cerenkov counters (C1, C2 and C3, C4). In addition, steel-scintillator assemblies at the end of each arm were used as rough hadron calorimeters. A number of scintillation counter hodoscopes were used in the trigger to help in the selection of elastic events. The "ring" and "wedge" shape of these hodoscopes enabled events to be selected with approximately the correct opening angles and coplanarity, respectively. The "prompt" hodoscopes PH1 and PH2 were used to form the first fast trigger. These hodoscopes were made from a total of 180 elements with sizes ranging from 15 x 15 cm^2 to 30 x 30 cm^2. They had a very good timing resolution (using zero-crossing discriminators) of approximately 1·2 ns[2]. A first coincidence between the two arms was formed in a matrix using correlations from elastic scattering kinematics.

Typically, about 200 triggers per burst were read into the computer and recorded on magnetic tape. A hard-wired processor, which used information from the multiwire proportional chambers to compute coplanarity and opening angle, was used for some of the runs. This device filtered the events before they were read into the on-line computer and so reduced the dead-time and the number of events recorded on magnetic tape.

In the off-line analysis the elastic events were selected on the basis of geometric and kinematic fits. The elastic events were seen very cleanly using this method and it is estimated that there is less than 5% contamination from the inelastic background. At 20 GeV/c incident momentum, in the large-angle acceptance region of the apparatus ($6 < -t < 20 (GeV/c)^2$), 104 pion-proton elastic events have been found (66 in π^+ - p and 38 in π^- - p elastic channels). A further 26 large-angle π^- - p events have been obtained

in the 30 GeV/c data. Corrections have been applied for detector efficiencies, reconstruction efficiencies, random veto losses, the muonic fraction in the beam and hydrogen target absorption.

The overall absolute normalization was checked by studying a small sample of proton-proton elastic events and comparing these with the previously published data in the same energy region[3]. The agreement is satisfactory and it is estimated that the overall systematic normalization error is ± 10%.

The resulting differential cross-sections for $\pi^- - p$ at 20 and 30 GeV/c and for $\pi^+ - p$ elastic scattering at 20 GeV/c incident momenta are shown in figures 2 and 3. The lower energy (or smaller angle) previously published data[1,4] are also shown in the figures for comparison.

DISCUSSION OF RESULTS

1. Dimensional Counting Rule

Within the framework of a constituent model, it is expected that the differential elastic cross-seciton at large momentum transfer, will take the form as $s \to \infty$

$$\frac{d\sigma}{dt} \propto \frac{1}{s^n} \; f\,(\cos\theta_{cm}) \qquad (1)$$

where n is given as the sum of the number of 'active' constituents in the hard scatter. This scaling at fixed angle has been predicted from field theory[5], scale invariance arguments[6] and from form factor considerations[7]. For $\pi^{\pm} - p$ elastic scattering, n should take the value 8.

Using the $\pi^- - p$ data at 9.7/9.8 GeV/c from ref 1, and the 20 and 30 GeV/c data from this experiment, ($19\ \text{GeV}^2 < s < 56\ \text{GeV}^2$), the form of $d\sigma/dt$ given in equation 1 can be fitted for $0.00 < \cos\theta_{cm} < 0.45$ with a value of $n = 9.5 \pm 0.5$ (suggesting some incompatibility with the counting rule), and in the smaller angle region $0.45 < \cos\theta_{cm} < 0.6$, with a value $n = 8.0 \pm 0.3$, (consistent with the counting rule). However, including

the systematic normalization errors between different experiments increases the error on n to ± 1.0 and ± 0.7, respectively.

For $\pi^+ - p$ elastic scattering, we only have data at 10[1] and 20 GeV/c (from this experiment), but these are consistent with an s^{-n} dependence with $n = 8.3 \pm 0.3$.

2. Constituent Interchange Model (CIM)

Using the specific version of this model due to Blankenbecler, Brodsky and Gunion[8], definite predictions for the form of the $f(\cos\theta_{cm})$ in equation 1 and hence of the differential cross-sections can be made as follows:

$$\frac{d\sigma}{dt}(\pi^+ - p) = \frac{\sigma 0}{s^8} \frac{1+z}{(1-z)^4} (4\alpha(1+z)^{-2} + \beta)^2 \qquad (2)$$

$$\frac{d\sigma}{dt}(\pi^- - p) = \frac{\sigma_0}{s^8} \frac{1+z}{(1-z)^4} (4\beta(1+z)^{-2} + \alpha)^2 \qquad (3)$$

where $z \equiv \cos\theta_{cm}$ and α and β are factors which can be taken as 2 and 1 respectively[8]. σ_0 is an overall unpredicted normalization factor. Fits to the earlier published data for 10 GeV $\pi^+ - p$ and 9.8 GeV $\pi^- - p$[1] give values of σ_0 of 0.5×10^{-24} cm^2 GeV^{14} and 1.6×10^{-24} cm^2 GeV^{14} respectively. There are, therefore, either difficulties of normalization between these two earlier experiments or a discrepancy with the theory.

In figures 2 and 3, the full curves are simultaneous fits to the new 20 and 30 GeV/c data to the forms given in equations 2 and 3. The fitted value of σ_0 is $4.4 \pm 0.5\ 10^{-25}$ cm^2 GeV^{14}. The curves at 9.7/9.8 GeV/c for $\pi^- - p$ and 10 GeV/c for $\pi^+ - p$ are computed from the higher energy fits. It can be seen that although the qualitative features are satisfactory, the relative normalizations of the predicted cross-sections are not in good agreement with the measured distributions at 10 GeV/c for $\pi^+ - p$ and 9.7/9.8 GeV/c for $\pi^- - p$. Also, the predicted curves at 20 and 30 GeV/c for $\pi^- - p$ are not steep enough to fit the data well.

3. Model of Preparata and Soffer

Recently Preparata and Soffer have carried out a calculation of large angle meson-baryon elastic scattering (see figures 2 and 3) in the framework of a theoretical approach where the quark degrees of freedom are permanently confined[10]. The basic elements of these calculations are baryon and meson wave functions in terms of quarks, qq and qqq scattering amplitudes, whose descriptions at high energy and at large angles (i.e. short distances) turn out to be rather simple. Their results for $\pi^{\pm}-p$ scattering are not dramatically different from the predictions of other generally accepted approaches like CIM[8]. For $\pi^{-}-p$, their predicted curve is less steep than that of the CIM model, (see figure 3). (However, in the case of $K^{\pm}-p$ scattering they yield very distinct predictions[10,11]).

CONCLUSIONS

The dimensional counting rule for the elastic $\pi^{\pm}-p$ channels is approximately satisfied. There is some suggestion, in the $\pi^{-}-p$ case, of a somewhat steeper energy dependence, for $\cos\theta_{cm} < 0.45$, than that predicted by the rule. The CIM model gives a good description of the broad features of the $\pi^{\pm}-p$ elastic differential cross-sections, but there is a discrepancy in the overall normalizations and in the steepness of the predicted curves at smaller angles for the $\pi^{-}-p$ case. In addition, the data can be qualitatively well represented by the model of Preparata and Soffer.

ACKNOWLEDGMENTS

We are grateful for the technical help and assistance given by R. Kiesler, B. Mouellic, R.H. Watson, D.B. Webb, G. Dromby, J.C. Lacotte, J.C. Le Marec, G. Barisone, S. Bianconi, A. Morelli, P. Poggi and L. Traspedini. In addition, we would like to thank many members of the support staff at CERN, including the SPS Experimental Support group, the DD on-line Support group (particularly A.J. Bogaerts) and the EP Electronics group.

REFERENCES

1) $\pi^+ - p$ 10 GeV/c, C. Baglin et al., Nucl. Phys. B98 (1975) 365.
$\pi^- - p$ 9.7, 9.8 GeV/c, D.P. Owen et al., Phys. Rev. 181 (1969) 1794.

2) M. Poulet and A. Santroni, Nucl. Instrum. Methods 148 (1978) 359.

3) J.V. Allaby et al., Phys. Letters 25B (1967) 156.

4) P. Cornillon et al., Phys. Rev. Letters 30 (1973) 403.

5) S.J. Bordsky and G.R. Farrar, Phys. Rev. Letters 31 (1973) 1153.

6) V.A. Matveev, R.M. Muradyan and A.N. Tavkhelidze, Nuovo Cimento Letters 7 (1973) 719.

7) M. Creutz and L.L. Wang, "The Gell-Mann Low equation and on-mass-shell amplitudes" BNL 19078 (1974) unpublished.

8) R. Blankenbecler, S.J. Brodsky and J.F. Gunion, Phys. Letters 39B (1972) 649 and Phys. Rev. D8 (1973) 287.

9) D. Sivers et al., Phys. Reports 23C (1976) 1.

10) G. Preparata and J. Soffer, submitted to Phys. Letters.

11) R. Almas et al., submitted to Phys. Letters.

Figure captions

Fig. 1 Experimental Layout.

C1 - C4 Atmospheric Cerenkov counters

CH1 - CH6 Multiwire proportional chambers

PH1 - PH2 "Prompt scintillaiton counter hodoscopes"

M Spectrometer magnet.

Fig. 2 Differential cross-section of $\pi^+ - p$ elastic scattering.
Data at 20 GeV/c from this experiment, at 10 GeV/c from ref. 1.

Fig. 3 Differential cross-section of $\pi^- - p$ elastic scattering.
Data at 20 and 30 GeV/c from this experiment, 9.71, 9.84 GeV/c from ref. 1, 22.6 GeV/c from ref. 4.

Experimental Layout.

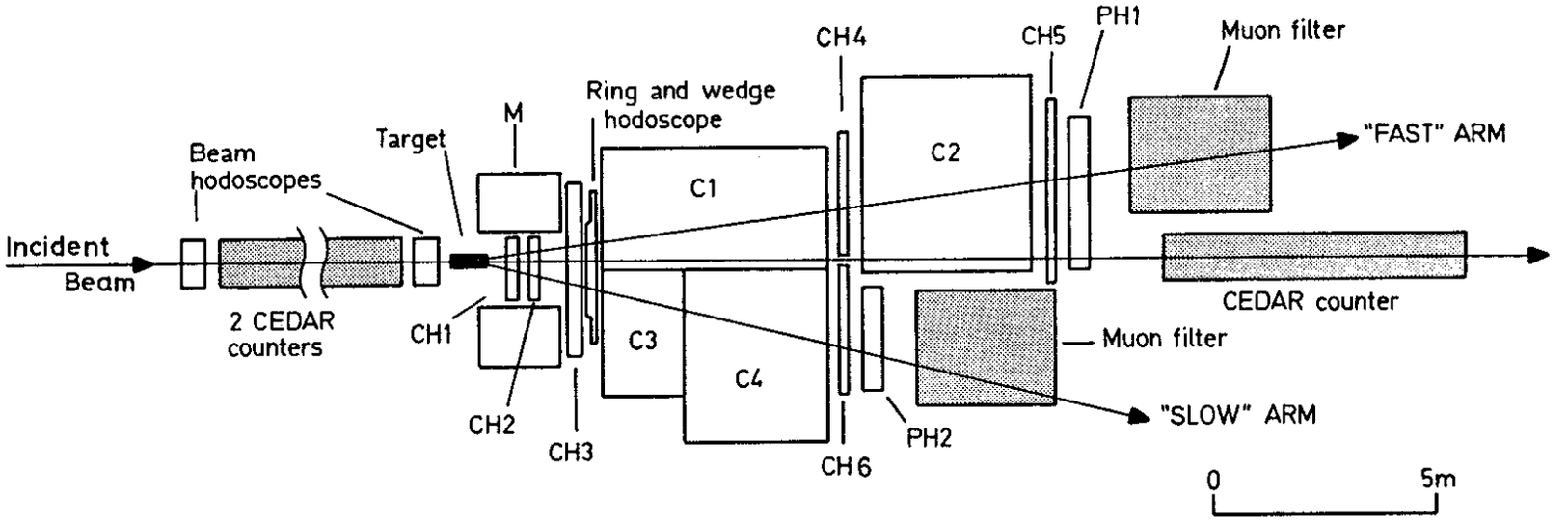

Fig. 1

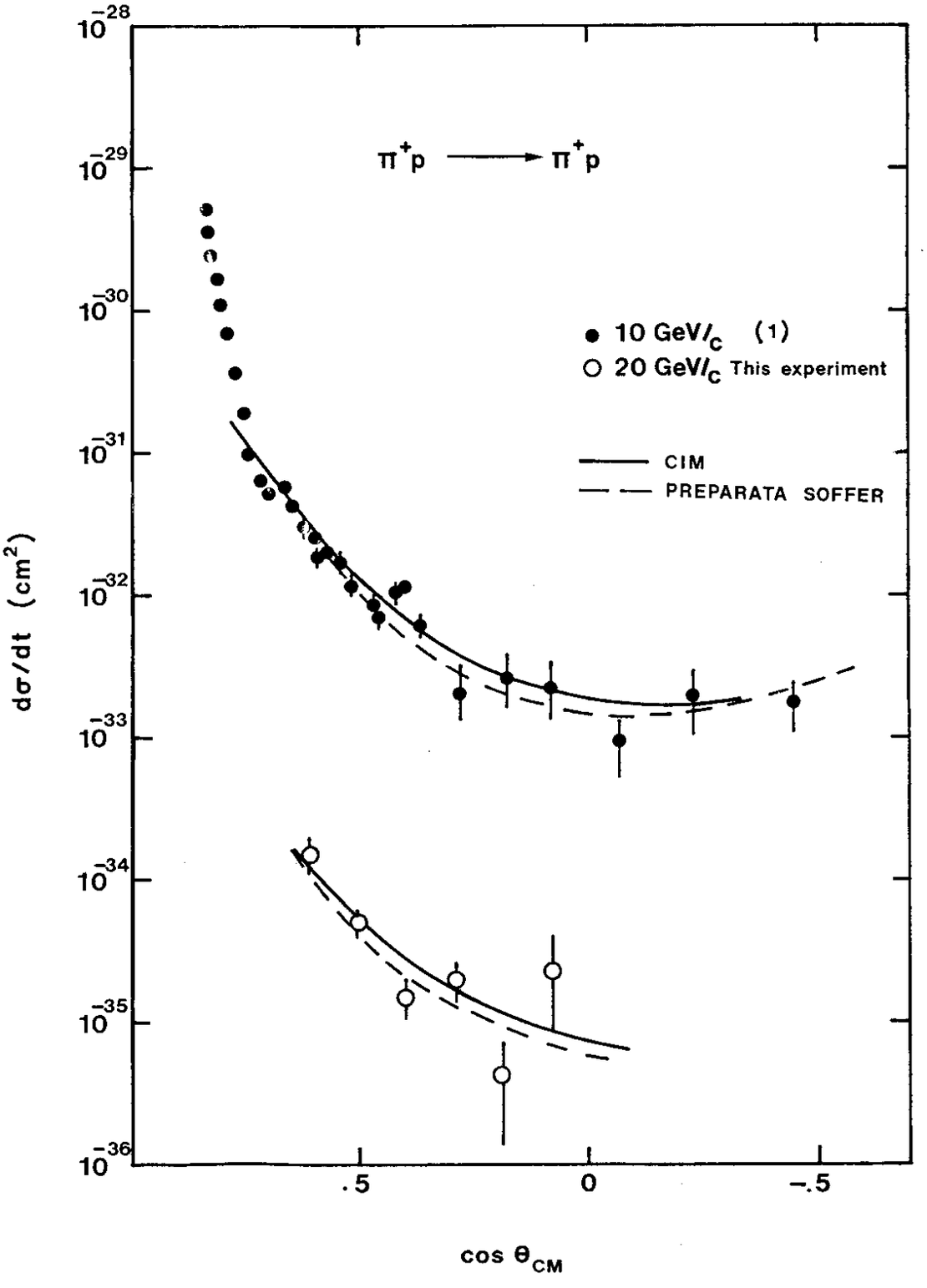
$\pi^+p \longrightarrow \pi^+p$
● 10 GeV/c (1)
○ 20 GeV/c This experiment
CIM
PREPARATA SOFFER
$d\sigma/dt$ (cm^2)
10^{-28}
10^{-29}
10^{-30}
10^{-31}
10^{-32}
10^{-33}
10^{-34}
10^{-35}
10^{-36}
.5
0
-.5
cos θ_{CM}

Fig. 2

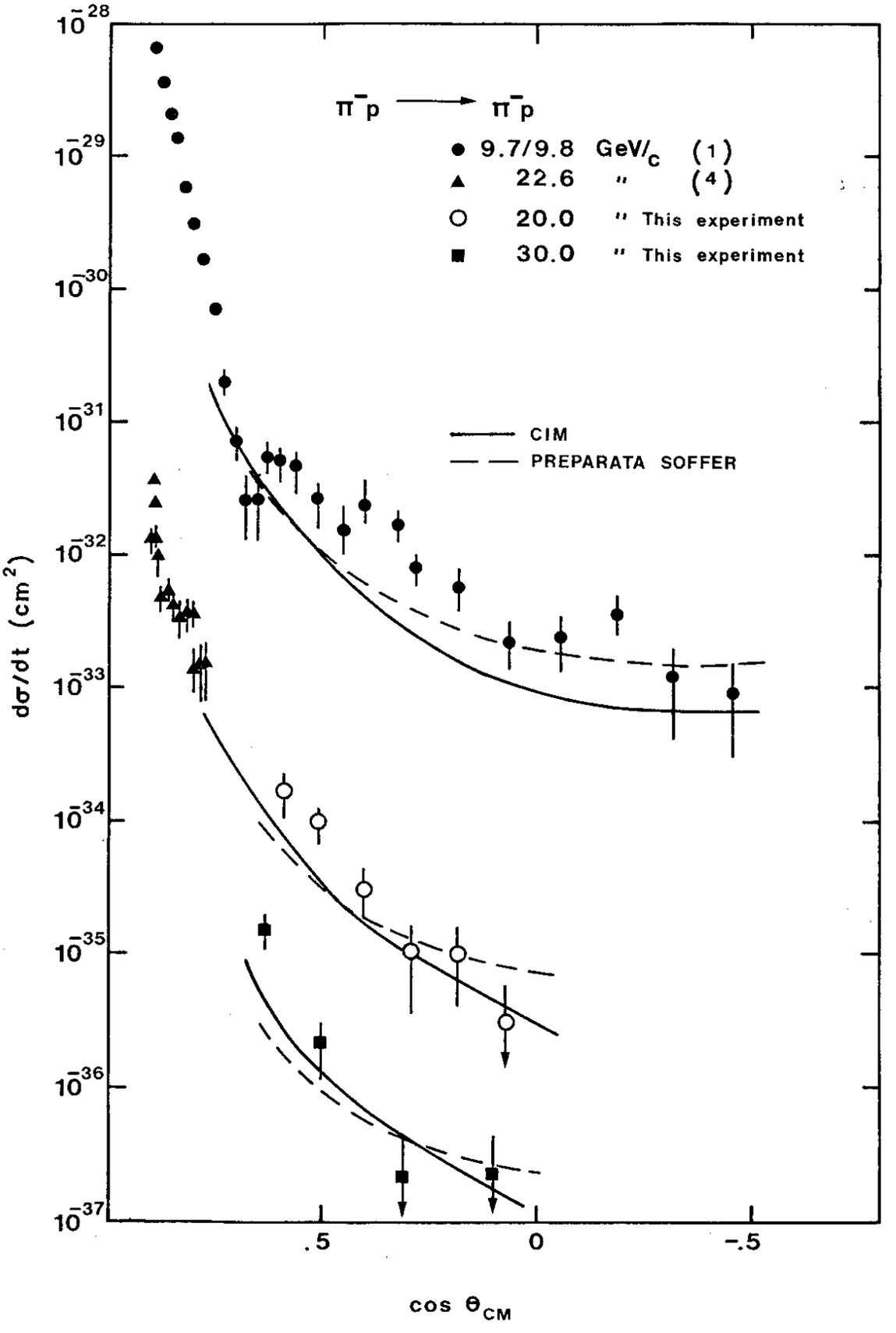
$\pi^- p \longrightarrow \pi^- p$
9.7/9.8 GeV/c (1)
22.6 " (4)
20.0 " This experiment
30.0 " This experiment
CIM
PREPARATA SOFFER
$d\sigma/dt$ (cm^2)
10^{-28}
10^{-29}
10^{-30}
10^{-31}
10^{-32}
10^{-33}
10^{-34}
10^{-35}
10^{-36}
10^{-37}
.5
0
-.5
cos θ_{CM}

Fig. 3